Nd-ordering-driven Mn spin reorientation and magnetization reversal in the magnetostructurally coupled compound $NdMnO_3$

A. Kumar,[1] S. M. Yusuf,[1,*] and C. Ritter[2]

[1]*Solid State Physics Division, Bhabha Atomic Research Centre, Mumbai 400085, India*

[2]*Institut Laue-Langevin, Boite Postale 156, 38042 Grenoble Cedex, France*

(Received 12 November 2016; revised manuscript received 3 June 2017; published 20 July 2017)

A detailed neutron diffraction study on $NdMnO_3$ infers that the low temperature transition at 15 K is due to the ordering of Nd sublattice moment with a $(0,-F_y,0)$ type spin arrangement. Interestingly, the ordering of the Nd sublattice drives a reorientation (by 180°) of the net ferromagnetic moment of the Mn sublattice along the b axis. Such a Mn spin reorientation from $(A_x, F_y, 0)$ (with an antiferromagnetic ordering temperature of 73 K) to $(A_x,-F_y,0)$ at 15 K, explains the magnetization reversal phenomenon present in this perovskite compound at 15 K. Moreover at 15 K, significant crystallographic structural distortions in terms of temperature variations of lattice parameters and bond angles are found. A sign change in the temperature variation of magnetic entropy is also found at 15 K. The present study signifies the role of rare-earth (Nd) moment ordering in tuning various physical properties, such as magnetocaloric and magnetoelastic of the larger size (>0.912 Å) R ion based $RMnO_3$ compounds.

DOI: 10.1103/PhysRevB.96.014427

I. INTRODUCTION

The perovskites ABO_3 are an important class of compounds that show a multitude of physical properties, such as superconductivity [1], colossal magnetoresistance (CMR) [2], ionic conductivity [3], photovoltaics [4], ferroelectricity [5], piezoelectricity [6], and novel magnetism involving spin, orbital, and charge ordering [7]. Such properties are of great importance in fundamental science and practical applications. Particularly, in rare-earth (R) manganites, $RMnO_3$, the transition metal ions (Mn, Fe, etc.) and their oxidation states play crucial roles in controlling their various magnetic and electric properties, viz. spin dependent transport [8], multiferroic behavior [9], half-metallic ferromagnetism [10], and charge and orbital ordering [11]. The R ions of different sizes, on the other hand, help to access different regimes of structural modulations [12] in $RMnO_3$ compounds; which in turn dictate many physical phenomena, such as magnetoelectric effect, spin reorientation, and magnetoelastic effect. Apart from controlling the structural modulations, low temperature magnetic ordering of rare-earth ions in $RMnO_3$ (R = Yb, Ho, Er, Eu, Dy, Gd, Tb, Sm) compounds [9,13–18] introduces finite and anisotropic f-d exchange interactions that affect the delicate balance of charge, orbital, and spin ordering in $RMnO_3$ compounds. Such f-d exchange interactions can also affect the magnetoelectric coupling found in many multiferroic $RMnO_3$ compounds [19]. For example, neutron diffraction study in orthorhombic $DyMnO_3$ multiferroic compound infers that Dy moment ordering plays an active role in controlling its ferroelectric polarization [20]. Besides, strong f-d (between paramagnetic rare-earth and magnetically ordered 3d transition metal ions) exchange interactions in several hexagonal $RMnO_3$ (R = Ho, Yb, and Er) manganites lead to Mn spin reorientation transition below the ordering temperature (T_N) of Mn moments [9]. In a similar manner, R moment ordering also is expected to cause (further) reorientation of Mn spins in $RMnO_3$ compounds. However, such a spin reorientation, due to ordering of R moments, has been reported only for the hexagonal $RMnO_3$ compounds with smaller size R ions (R: Ho, Er, and Yb) [9,21]. In the present work, we have observed a clear evidence of Mn spin reorientation transition at Nd moment ordering (15 K) in an orthorhombic $NdMnO_3$ compound. Our study also provides a microscopic understanding of the observed magnetization reversal phenomenon (in a field-cooled dc magnetization study) at the Nd moment ordering in $NdMnO_3$ compound. Such compounds showing the magnetization reversal phenomenon have technological potential for device applications, such as thermally assisted magnetic random access memories, bipolar magnetocaloric, and spin resolving devices [22–31]. In the present study we bring out the role of Nd moment ordering in explaining technologically important spin reorientation and magnetization reversal phenomena in $NdMnO_3$.

$NdMnO_3$ shows a variety of interesting physical and chemical properties, such as phase segregation and nonideal oxygen stoichiometry [32–40], positive and negative exchange bias [41], negative magnetization involving magnetization reversal [33–37,41], and magnetoelastic effect [42]. This manganite compound also exhibits a sizable magnetocaloric effect [43] with magnetic entropy change ($-\Delta S_m$) reaching a maximum of ∼4 J/kg K (under 50 kOe magnetic field) at low temperatures. The magnetocaloric effect is more pronounced in nanoparticles of $NdMnO_3$ [43].

$NdMnO_3$ possesses an orthorhombic (space group: *Pnma* or equivalent space group *Pbnm*) crystal structure [38,42,44–49] at room temperature, and undergoes a first order Jahn-Teller (JT) phase transition from an orbitally ordered phase to an orbitally disordered phase with increasing temperature (T_{JT}) around 600 − 800 °C [50]. Moreover, the compound is reported [45,51] to show a sharp drop of the electrical resistivity and thermoelectric power above the T_{JT}. This drop is associated with the transition from the cooperative JT ordered phase (below T_{JT}) to a disordered phase with fluctuating JT distortions where phonon assisted conductivity enhancement is reported [51]. Though the compound shows a variety of such interesting physical properties, it does not show any

*Corresponding author: smyusuf@barc.gov.in

ferroelectric order (in contrast to other RMnO$_3$ perovskites [52], R: Tb, Dy, Eu).

The reported dc magnetization [33–36,41,47,53], ac susceptibility [45,46,48,53], and specific heat data [48,54] indicate that a magnetic phase transition occurs around 75 K (T_C) in NdMnO$_3$. Neutron diffraction experiments [35,38,42,47] reveal that this transition corresponds to the ordering of the Mn sublattice with (A_x, F_y, 0; *Pnma* setting) type spin arrangement. The Mn moments are antiparallel in two adjacent *ac* planes, and a net ferromagnetic (FM) moment appears along the *b* axis. Another peak in the ac susceptibility [45,46,48,53] as well as in the heat capacity data [48,54] is reported at a lower temperature around 15 K indicating a second magnetic transition in NdMnO$_3$. However, there are conflicting reports about this low temperature magnetic transition. Even strikingly dissimilar results are reported in different zero-field (ZF) neutron diffraction studies. For example, Wu *et al.* [46,55] have concluded that the low temperature transition corresponds to the reorientation of the Mn spins, and no evidence of the Nd ordering is seen down to 1.8 K. On the other hand, Muñoz *et al.* [47] and Mihalik *et al.* [38] have reported an ordering of the Nd sublattice around 15 K with a FM arrangement of the Nd and Mn moments. Chatterji *et al.* [42] have inferred an *A*-type antiferromagnetic (AFM) order of Mn moments around 80 K, whereas a FM component in Mn moments develops only when the Nd moment orders around 15 K. On the other hand, the x-ray magnetic circular dichroism (XMCD) measurements [37] (under 1 and 50 kOe fields) infer a FM coupling between the Mn and Nd moments in the entire temperature range below the T_C (∼75 K) of this compound. Here we stress upon the fact that the reported low temperature transition does not depend on the sample preparation conditions as the contradicting reported results on "NdMnO$_3$" are independent of the sample stoichiometry. In fact, both magnetic transitions are reported in the stoichiometric [41–43,46–48,55] as well as in the off-stoichiometric compounds, viz. NdMnO$_{3+\delta}$ [38,53], Nd$_{0.93}$MnO$_{2.96}$ [34,35], Nd$_{0.9}$MnO$_y$ ($2.85 \leqslant y \leqslant 2.93$) [33], and NdMnO$_{3.11}$ [36,37].

Most interestingly, the low temperature magnetic transition around 15 K coincides with the appearance of a magnetization reversal [22] in field-cooled dc magnetization studies where the temperature dependent magnetization changes its sign at the magnetic compensation temperature (T_{Comp}) of ∼15 K. Such a magnetization reversal has been reported in off-stoichiometric Nd$_{0.9}$MnO$_{3-\delta}$ [33,40], Nd$_{0.93}$MnO$_{2.96}$ [34,35], NdMnO$_{3.11}$ [36,37] as well as stoichiometric NdMnO$_3$ [41] compounds. However, an explanation of the negative magnetization has been elusive so far. For example, Ihzaz *et al.* [34,35], on the basis of ZF neutron diffraction study, have concluded that a rearrangement of the Mn sublattice moments of the two phases (viz. NdMnO$_3$ and Nd$_{0.9}$MnO$_3$) of Nd$_{0.93}$MnO$_{2.96}$ compound around the Nd sublattice ordering temperature results in a negative magnetization. On the other hand, Bartolomé *et al.* [36,37], using ZF neutron diffraction and field-dependent XMCD studies, have interpreted the magnetization reversal in phase segregated NdMnO$_{3.11}$ as a consequence of slow dynamics of FM (oxygen-rich) clusters, which are antiferromagnetically coupled with the (oxygen-poor) canted-AFM matrix at low temperatures. Field-cooled dc magnetization study by Hong *et al.* [41] have shown the presence of the magnetization reversal as well as of an exchange-bias reversal in the stoichiometric NdMnO$_3$ compound. The authors have conjectured that the AFM coupling between the Nd moments and the FM Mn moments causes a negative magnetization in the NdMnO$_3$ compound. A detailed investigation of the magnetization reversal phenomenon in the NdMnO$_3$ system is, therefore, required.

We have, therefore, employed ZF neutron diffraction along with field-cooled (10 Oe) neutron depolarization [56,57] to gain a microscopic as well as mesoscopic understanding of the low temperature magnetic ordering and its relation to the magnetization reversal phenomenon in NdMnO$_3$. In our present study on the stoichiometric NdMnO$_3$ compound, we will show that the Mn sublattice orders with a (A_x, F_y, 0) or equivalent (A_x, $-F_y$, 0) spin arrangement at 73 K, whereas the Nd sublattice ordering at 15 K with a (0, $-F_y$, 0) spin arrangement is accompanied by the reorientation of the Mn spins from (A_x, F_y, 0) to (A_x, $-F_y$, 0). The magnetic ordering of the Nd moments, coupled with the Mn spin reorientation, induces the magnetization reversal in NdMnO$_3$. Additionally, consequences of the Nd ordering on the magnetocaloric effect and on the structural distortions are revealed. The observed magnetostructural effects, produced by spin-lattice coupling, bear importance for the explanation of the multifunctional properties of perovskites. In particular, the present study reveals the importance of the unique observation of the rare-earth moment ordering and its consequence on the Mn spin reorientation with regard to all other RMnO$_3$ compounds with ionic size of R ions larger than 0.912 Å.

II. EXPERIMENT

The polycrystalline NdMnO$_3$ compound was prepared by solid state reaction method. A stoichiometric mixture of Nd$_2$O$_3$ and MnO$_2$ was heated initially at 1000 °C for 12 h, and then allowed to cool down to room temperature. Following this, the sample was ground, palletized and then heated at 1300 °C for 60 h in a carbolite furnace. The single phase crystalline nature of the compound was confirmed by x-ray diffraction (not shown). In order to study the crystal structure of the compound, room temperature neutron-diffraction data were recorded using the high-resolution powder diffractometer, D2B ($\lambda = 1.594$ Å) at the Institut Laue Langevin (ILL), Grenoble, France, whereas the evolution of the magnetic ordering was studied by recording high intensity thermal diffractograms using the high flux neutron diffractometer, D1B ($\lambda = 2.52$ Å) as well at ILL. Neutron depolarization experiments were carried out using the polarized neutron spectrometer at Dhruva reactor, Trombay, Mumbai, India. For diffraction measurements, a liquid helium cryostat was used, whereas a closed cycle helium refrigerator (CCR) was used for depolarization measurements. For depolarization measurements, the sample was cooled down to 5 K in a 10 Oe field applied in the direction of incident neutron beam polarization. The transmitted neutron beam polarization was measured in the warming cycle by keeping the 10 Oe field "ON." dc magnetization of the compound was measured in both the zero field-cooled (ZFC) and field-cooled (FC) conditions as a function of temperature down to 5 K and magnetic field up to 50 kOe using a commercial vibrating sample magnetometer. The ac susceptibility measurements

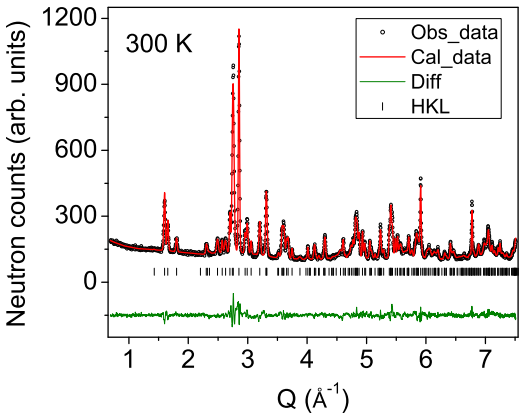

FIG. 1. Rietveld refined neutron diffraction pattern (at 300 K, $\lambda = 1.594$ Å) of $NdMnO_3$. The observed and fitted patterns are shown by open circle (o) and solid line, respectively, and their difference is plotted at the bottom. The short vertical lines represent the positions of nuclear Bragg peaks under the *Pnma* (No. 62) space group. Here $Q\{= (4\pi \sin\theta)/\lambda;\ \theta = \text{Bragg angle}\}$ is the magnitude of the scattering vector.

were carried out as a function of temperature down to 5 K using a commercial ac-susceptibility probe.

III. RESULTS AND DISCUSSION

A. Crystal structure

Figure 1 shows the Rietveld [58] refined room temperature neutron diffraction pattern, recorded using the high resolution diffractometer D2B. The crystal structure is indexed to an orthorhombic phase (space group: *Pnma*) with lattice constants $a = 5.6967(2)$ Å, $b = 7.5873(1)$ Å, and $c = 5.4097(1)$ Å; as reported in previous studies [34,38,44,46,47]. The Nd and Mn cations occupy the 4c (x, 1/4, z) and 4b (0, 0, 1/2) crystallographic positions, respectively, whereas the oxygen anions occupy the 4c (x, 1/4, z) and 8d (x, y, z) crystallographic positions. The Rietveld analysis infers the stoichiometric (3.00 ± 0.01) value of oxygen content. The thermogravimetric analysis (not shown) over a temperature range of $50 - 1200\,^{\circ}$C on the present sample infers that the maximum variation of oxygen content (δ) is ± 0.03. The structural refinement has been carried out by considering the strain model No. 3 in the Rietveld refinement method [58]. The strain is found to be maximum for the (400) Bragg plane. We can exclude, for our sample, the two phase scenario as reported by Ihzaz *et al.* [34,35], as a structural refinement assuming the two phases, viz. $NdMnO_3$ and $Nd_{0.9}MnO_3$, resulted in a poorer fit of the diffraction data. Moreover, a fitting of the neutron diffraction data in a structure with lower symmetry (monoclinic, space groups: $P2_1/c$ and $P2_1/m$) [53,59] did not result in any improvement in the goodness of fit (χ^2). Hence, the orthorhombic structure (space group: *Pnma*) is used for all the subsequent neutron diffraction data analysis.

B. Magnetic ordering

1. dc magnetization and ac susceptibility

The FC dc magnetization curves, under different cooling magnetic-fields (H), are depicted in Fig. 2(a). The large growth

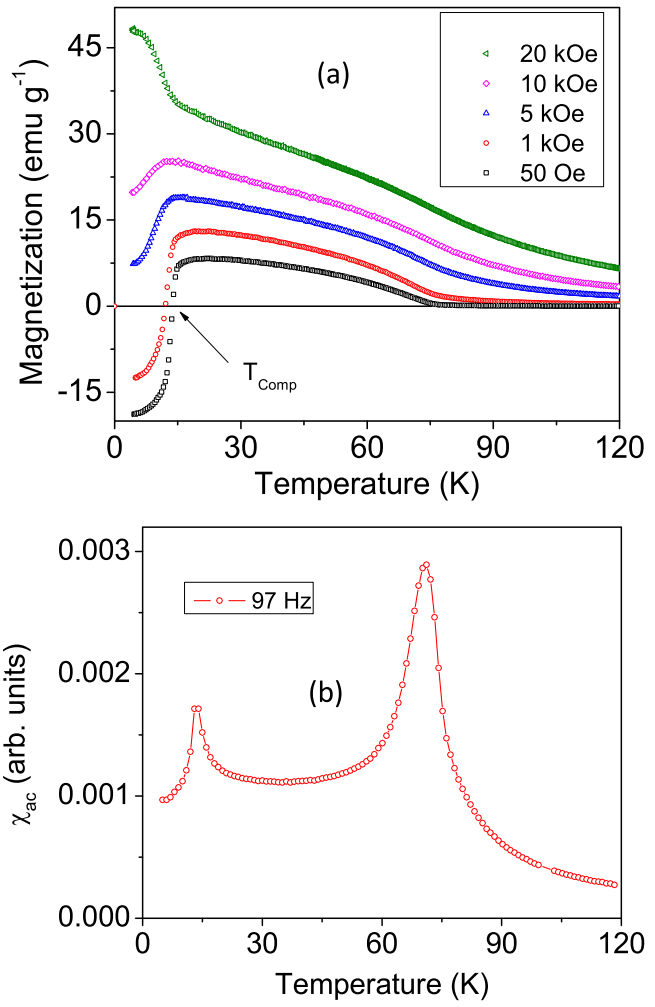

FIG. 2. (a) Field-cooled dc magnetization curves at various cooling fields showing negative magnetization below ~15 K for $H \leqslant 1$ kOe. (b) Real part of ac susceptibility (χ_{ac}) curve at 97 Hz, showing two magnetic transitions at 73 and 15 K, respectively.

of magnetization below ~ 75 K (under low applied field) indicates the onset of magnetic ordering [36,41,47]. Interestingly, the temperature dependent magnetization for $H \leqslant 1$ kOe starts decreasing below 20 K, and becomes negative (opposite to the measurement field) below the compensation temperature (T_{Comp}) of ~ 15 K. For $H > 1$ kOe, the magnetization remains positive throughout the measured temperature range, however, a down turn is observed around the T_{Comp} until $H > 10$ kOe. Both magnetic transitions also have their signatures in the ac susceptibility (χ_{ac}) curve, depicted in Fig. 2(b). The presence of a huge peak in the real part of χ_{ac} around 73 K indicates the development of bulk magnetic ordering in $NdMnO_3$ [46]. At a lower temperature of around 15 K, a small peak is seen, and it has been interpreted in the literature either as a signature of a Mn spin reorientation [46,55] or of the Nd sublattice [36,47] ordering. The coincidence of this low temperature magnetic transition with the occurrence of the magnetization reversal [Fig. 2(a)] can be clearly seen. In order to resolve the nature of low temperature magnetic transition, experimental tools, such as neutron diffraction and neutron depolarization are very

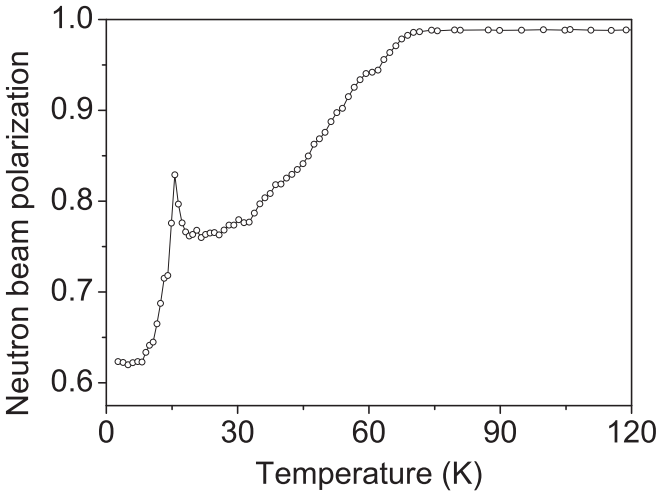

FIG. 3. Transmitted neutron beam polarization curve for $NdMnO_3$ compound.

much essential, and have, therefore, been employed by us to get a clear understanding of magnetic ordering at the atomic as well as at the domain level.

2. Neutron depolarization

Neutron depolarization measurements (Fig. 3) have been carried out in the temperature range of 3–140 K. In a neutron depolarization experiment [56,57,60], a polarized neutron beam is made to pass through a sample, and the transmitted neutron beam polarization is recorded as a function of temperature. During the passage, the magnetic moments of the polarized neutrons precess around the local magnetic field of randomly oriented magnetic domains resulting in a loss of neutron beam polarization. Such a neutron depolarization experiment gives a fairly good estimate of the temperature evolution of magnetization as well as of the size of magnetic domains/clusters [13,61–66]. The observed decrease in the neutron beam polarization below 73 K infers a magnetic ordering in $NdMnO_3$ with nonzero domain magnetization. Below 20 K, the neutron beam polarization shows an incomplete recovery in the form of a peak with a maximum around 15 K which coincides with the low temperature peak in the χ_{ac} curve [Fig. 2(b)] as well as with the T_{Comp} in the dc magnetization curves [Fig. 2(a)] for $H \leqslant 1$ kOe. Below 15 K, the neutron beam gets further depolarized with lowering of temperature. The recovery of the neutron beam polarization around 15 K indicates a net decrease in the magnetic field integral (product of domain magnetization and domain size) of the individual magnetic domains [57]. As our neutron diffraction results (presented later) do not show any evidence of a decrease of the magnetic correlation length over this temperature range, only a net decrease in the individual domain magnetization can explain the decrease of the magnetic field integral at $T = T_{Comp}$. A full recovery of the neutron beam polarization at T_{Comp} cannot be observed due the temperature variation of the sample over the area (30 mm × 15 mm) exposed to the neutron beam. Temperature dependent neutron diffraction experiments, described below, have been carried out to shed light on the microscopic nature of the sublattice magnetic ordering inside domains, and consequently on the magnetic ordering at 15 K.

3. Magnetic neutron diffraction

High intensity neutron diffraction patterns [Fig 4(a)] have been recorded down to 1.5 K. The measured diffraction patterns [Fig 4(b)] have been analyzed by employing the Rietveld refinement using the Fullprof program [67]. The results of the Rietveld analysis infer that Mn moment orders at 73 K [Fig. 4(c)] as found in earlier studies [35,38,42,47]. A further change of the diffraction pattern is visible below 15 K where extra intensity can be found on the (200) and {(121) and (002)} Bragg reflections, while the (101) reflection decreases [Fig. 4(c)]. These changes could be related to a change of the magnetic order on the Mn sublattice or indicate the onset of the ordering of the Nd sublattice [47]. The magnetic models (as per the Bertaut [67] method) compatible with the *Pnma* crystal symmetry have been tested in order to determine the magnetic structure both below and above 15 K. A very good fit of the data is possible in the temperature range $T_N > T > 15$ K using the $(A_x, F_y, 0)$ or equivalent $(A_x, -F_y, 0)$ model with only the Mn sublattice being magnetically ordered while the Nd sublattice stays paramagnetic. This model corresponds to a canted AFM type ordering of the Mn sublattice, where the components of the Mn moments in *a*-*c* planes are coupled ferromagnetically, and the adjacent *a*-*c* planes are antiferromagnetically coupled along *b* axis. A net FM component of Mn moments appears along *b* axis due to canting. The ordered components of the moments at 20 K of the Mn sublattice are $m_a = 2.36(2)\,\mu_B$, $m_b = 1.2(1)\,\mu_B$, and $m_c = 0\,\mu_B$. Let us point us out here that it is not possible to discriminate between a $(A_x, F_y, 0)$ and a $(A_x, -F_y, 0)$ configuration. For the neutron diffraction patterns at 1.5 K, the analysis has been carried out assuming the following spin configurations for Mn and Nd, respectively, (i) $(A_x, -F_y, 0)$ and $(0, -F_y, 0)$, (ii) $(A_x, -F_y, 0)$ and no ordering, (iii) $(A_x, -F_y, 0)$ and $(0, F_y, 0)$, and (iv) $(A_x, F_y, 0)$ and $(0, F_y, 0)$, and the Rietveld fitted patterns are shown in Fig. 4(b) for model (i), and Fig. 5(a) for models (ii), (iii), and (iv). The magnetic model (i) results in the lowest value of magnetic *R* factor (= 8.6) in the Rietveld refinement [bottom panel of Fig. 4(b)]. It is quite evident from Fig. 5(a) that the magnetic model (ii) is not able to account for the intensities of the (101) and [(121)(002)] magnetic Bragg reflections properly (magnetic *R* factor = 10.3). The magnetic models (iii) and (iv) are also not able to account for the intensities of the [(121)(002)] and (210) magnetic Bragg reflections properly (magnetic *R* factor = 9.6 for both models). The accepted model (i) reveals that the ordering of the Nd sublattice with a $(0, -F_y, 0)$ type spin arrangement is imperatively accompanied by a $(A_x, -F_y, 0)$ type spin arrangement of the Mn moments. Due to the interaction of the two magnetic sublattices and the fact that the Nd site is noncentrosymmetric, it is now possible to discriminate this $(A_x, -F_y, 0)$ configuration from a $(A_x, F_y, 0)$ configuration. This result opens up the possibility to suggest that the direction of the net FM moment of the Mn and Nd sublattices below 15 K might be opposite [Figs. 5(b)–5(d)] to the net FM moment of the Mn sublattice above 15 K. The ordered moments at 1.5 K are $m_a = 2.44(1)\,\mu_B$, $m_b = -1.66(6)\,\mu_B$, and $m_c = 0\,\mu_B$ for the Mn sublattice; and $m_a = 0\,\mu_B$,

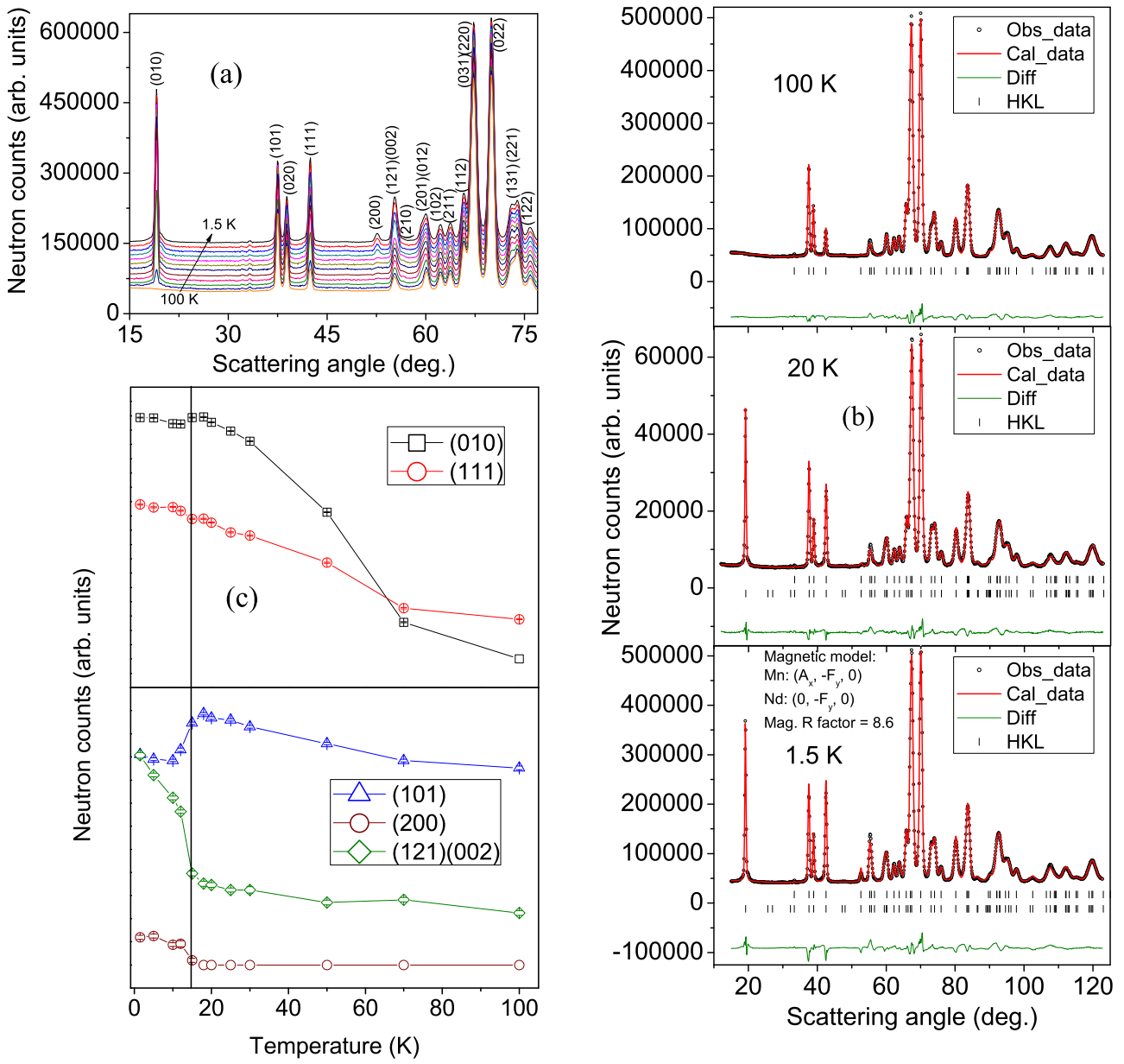

FIG. 4. (a) Neutron diffraction patterns ($\lambda = 2.52$ Å) of $NdMnO_3$ compound in the temperature range of 100–1.5 K in which patterns are shifted in the y axis for clarity. (b) Rietveld refined neutron diffraction patterns at 100, 20, and 1.5 K, depicting different magnetic ordering regimes in $NdMnO_3$ compound. The second vertical bars in the middle and bottom panels indicate the positions of magnetic Bragg reflections. (c) Thermal evolution of the main magnetic reflections in 100–1.5 K range.

$m_b = -1.06(6)\,\mu_B$, and $m_c = 0\,\mu_B$ for the Nd sublattice. We propose therefore that the low temperature (15 K) magnetic transition in $NdMnO_3$ compound is characterized by a FM ordering of Nd moments along with a reorientation (by 180°) of the net FM moment (due to both Mn and Nd) along the b axis. The temperature dependence of the derived magnetic moments is depicted in Fig. 5(b), and the derived magnetic structures above and below the Nd ordering temperature (20 and 1.5 K, respectively) are shown in Figs. 5(c) and 5(d).

C. Magnetization reversal

Now we explain the microscopic origin of the magnetization reversal as observed in the temperature dependent dc magnetization study across 15 K in Fig. 2(a). The neutron diffraction results infer an ordering of the Mn moments below 73 K with a net FM moment along b axis. The net FM moment aligns itself along the applied field direction, and a positive magnetization results down to 15 K in the dc magnetization measurement [Fig. 2(a)]. Our neutron diffraction data analysis clearly infers that the coupling between the F_y components of the two magnetic sublattices is ferromagnetic and that it can be determined to be in a definite direction (namely $-F_y$) relative to the A_x component of the Mn sublattice. The negative magnetization seen in the dc magnetization data below 15 K should be related to a net FM moment below 15 K (due to both Mn and Nd ions) being antiparallel to the net FM moment of Mn ions above 15 K. The driving

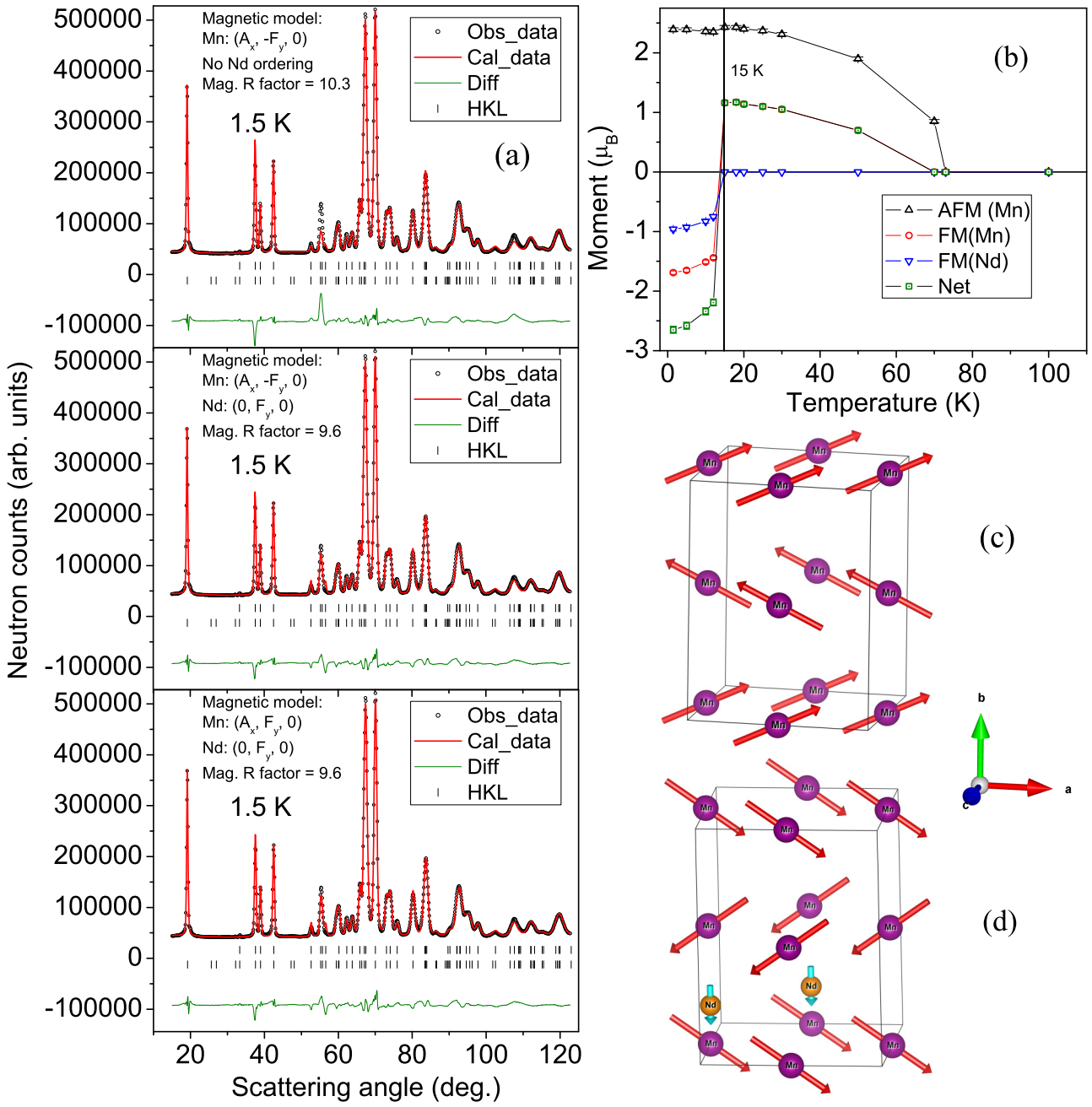

FIG. 5. (a) Rietveld refined neutron diffraction patterns at 1.5 K, with possible magnetic models as described in text. (b) Plot of the derived sublattice and net magnetic moments. (c) and (d) Magnetic structures at 20 and 1.5 K, respectively.

force for the magnetic ordering of the Nd moments to adopt the $(0, -F_y, 0)$ arrangement should be found in the magnetocrystalline anisotropy with a simultaneous change of the net FM moment of $NdMnO_3$ from a positive value (above 15 K) to a negative value (below 15 K). We stress upon the fact that though there are a large number of reports on the magnetization reversal in $NdMnO_3$ [33–37,41], an explanation of the origin of the phenomenon is still lacking as briefed in the Introduction. In the present work, based on the combined results of dc magnetization, neutron depolarization (both under finite magnetic field), and ZF neutron diffraction studies, we have observed a Mn spin reorientation transition at 15 K, driven by rare-earth (Nd) moment ordering, which provides a microscopic understanding of the observed magnetization reversal in the $NdMnO_3$ compound. It may be recalled here that Néel [68,69] in his seminal work on spinel ferrites predicted magnetization reversal in ferrimagnets under some special situations. Following this, the existence of such magnetization reversal has been reported experimentally in a variety of other magnetic compounds [22,24,70–73].

D. Spin reorientation

Now we discuss in more detail the origin and nature of the spin reorientation transition in $NdMnO_3$. A prerequisite for spin rotation is the presence of anisotropy. Spin

reorientation transitions have been studied extensively in perovskites [26,28,74–76]. Spin reorientation transitions are generally observed as a function of temperature below T_C. However, external stimuli, such as magnetic field [29] and laser [30] could also induce spin reorientation transition. The simultaneous spin ordering of the Nd sublattice and the postulated spin reorientation of the Mn sublattice in $NdMnO_3$ indicate that the spin reorientation could be induced by the onset of local magnetic exchange (f-d) interactions between Nd^{3+} and Mn^{3+} moments. It may also be noted that the Nd^{3+} ions at the 4c (x, 1/4, z) site occupy less symmetric position compared to the 4b (0, 0, 1/2) position occupied by Mn^{3+} ions. Because of the symmetry of 4b (0, 0, 1/2) site, the magnetic ordering of Mn^{3+} ions with (A_x, F_y, 0) or (A_x, $-F_y$, 0) type spin arrangements is equivalent as already mentioned above. However, for Nd^{3+} ions at the 4c (x, 1/4, z) site, the (0, $-F_y$, 0) type spin arrangement is preferred against the (0, F_y, 0) type spin arrangement due to symmetry considerations of the 4c site. Moreover, Nd^{3+}-O-Mn^{3+} exchange interactions are dominantly ferromagnetic as inferred from the analysis of the low temperature neutron diffraction data. The magnetic ordering of the Nd sublattice at ~15 K, thus, drives the spin reorientation transition. Similar spin reorientation transitions (involving Fe^{3+} ions), observed in $CaNdFeO_4$ and $SrNdFeO_4$ compounds [27,31], have been explained on the basis of the onset of the Nd sublattice magnetic ordering.

E. Magnetostructural coupling

The spin reorientation transition is correlated with marked structural distortions in $NdMnO_3$. Figures 6(a) and 6(b) depict the temperature variation of the lattice constants and Mn-O-Mn bond angles, respectively. The b and c lattice parameters as well as the Mn-O1-Mn and Mn-O2-Mn bond angles (mainly responsible for magnetic exchange interaction paths) show clear changes around 15 K. The Jahn-Teller distortion (Δ_{JT}) is defined as

$$\Delta_{JT} = [1/6]\sum_{n=1}^{6}[\{d_n - \langle d\rangle\}/\langle d\rangle]^2, \quad (1)$$

where $d_n(\langle d\rangle)$ is the individual (average) Mn-O bond length. The variation of Δ_{JT} as a function of temperature [inset of Fig. 6(b)] shows a large jump at ~15 K, indicating a large magnetostructural coupling. Earlier studies on $NdMnO_3$ (Chatterji *et al.* [42]) have mainly brought out a magnetostructural coupling at Mn ordering temperature (73 K), whereas our study has brought out the presence of an additional significant magnetostructural coupling at the Nd ordering temperature (15 K). The structural distortion is, essentially, the consequence of the spontaneous exchange striction associated with the magnetic ordering of the Nd sublattice at 15 K, and gives a microscopic understanding of the observed magnetization reversal in the temperature dependent dc magnetization data.

F. Magnetocaloric effect

Now we discuss the effect of magnetic ordering of Nd ions on the magnetocaloric properties of $NdMnO_3$ compound. The magnetocaloric effect (MCE) is the measure of the magnetic entropy change ($-\Delta S_m$) (Fig. 7), derived from the

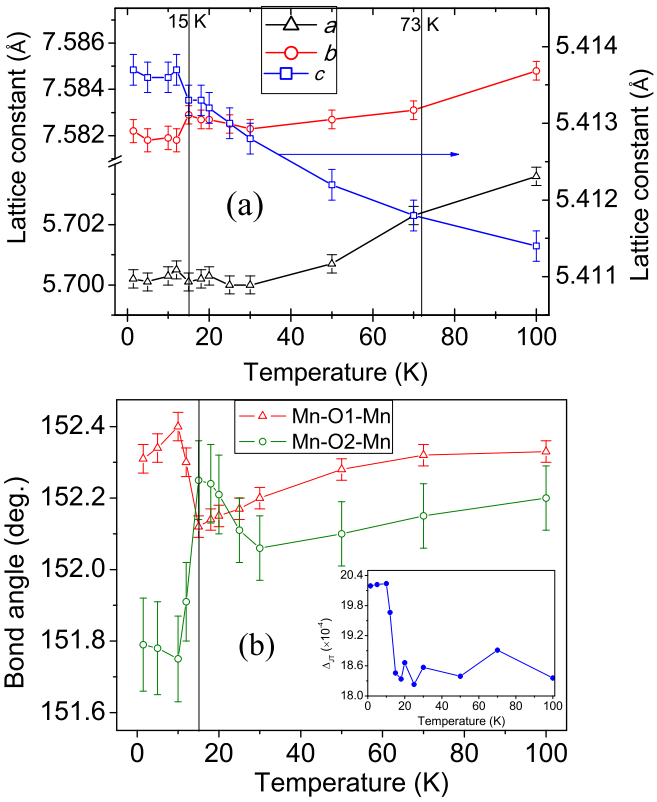

FIG. 6. Variation of (a) lattice parameters and (b) bond angles with temperature for $NdMnO_3$ compound. The inset in (b) depict the variation of the Jahn-Teller distortion (Δ_{JT}) as a function of temperature.

first derivative of magnetization with respect to temperature ($\partial M/\partial T$) upon application of magnetic field for a field change from H_i to H_f by using the following equation:

$$\Delta S_M(T)_{\Delta H} = \int_{H_i}^{H_f}\left(\frac{\partial M}{\partial T}\right)_H dH. \quad (2)$$

A steep increase of the absolute value of $[-\Delta S_M(T)]$ is found around the Nd sublattice ordering temperature, and it

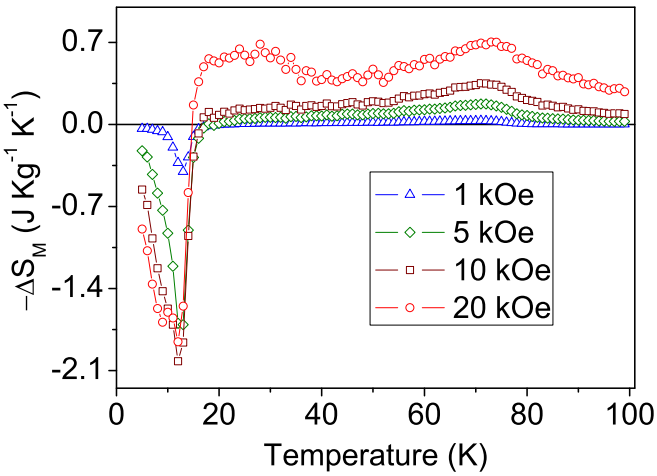

FIG. 7. Variation of magnetic entropy change ($-\Delta S_m$) for $NdMnO_3$ compound.

can be attributed to the rapid change in the magnetization of $NdMnO_3$ due to the Nd sublattice ordering. A small maximum of $(-\Delta S_m)$ is also found around the ordering of the Mn sublattice at $T = 73$ K. We have shown the consequence of the magnetization reversal phenomenon on the magnetocaloric properties of $NdMnO_3$ compound. We report a sign reversal of $(-\Delta S_m)$ around 15 K for the $NdMnO_3$ compound (Fig. 7), and it has implications in practical applications of magnetization reversal in the area of magnetic cooling [22].

We discuss now the importance of the present observations. The $RMnO_3$ compounds have been investigated extensively in the past and results can be found in the literature [9,16,17,77–79]. It was found that for the smaller size R ions (R: Ho, Er, and Yb), a Mn spin reorientation occurs at the magnetic ordering of the R ions. Namely, spin reorientation transitions at 4, 2.5, and 3.5 K have been observed with the ordering of the Ho, Er, and Yb ions, respectively, in the $RMnO_3$ compounds [9]. On the other hand, no such spin reorientations (of Mn) have been reported at the magnetic ordering of the R ions in $RMnO_3$ compounds with larger size (ionic radius >0.912 Å) R ions (R: Dy, Tb, Gd, Eu, and Sm) [16,18,80]. This could be explained by the structural and magnetic details varying with the size of the R ions. It is found that while the average Mn-O bond distances do not change significantly with the ionic size of R, the Mn-O-Mn bond angles (mainly responsible for the magnetic ordering of the Mn ions) as well as the octahedral distortions increase significantly with varying R ionic size [81]. It is therefore evident that the magnetostructural coupling is stronger at the rare-earth ordering in $RMnO_3$ compounds with smaller R ions. The present study represents a unique example where a spin reorientation could be established even with a larger R (=Nd; ionic radius 1.165 Å). This new finding is significant considering the fact that the $RMnO_3$ compounds with smaller R ions show a stronger coupling of the magnetoelectric, magnetoelastic, and thermoelectric properties at the rare-earth ordering [17,77,79,82], and it leads to the believe that a reinvestigation of the $RMnO_3$ compounds with larger R ions is needed. The present study should encourage us to investigate the role of rare-earth ordering and spin reorientations of transition metal ionic moments on magnetocaloric, thermoelectric, dielectric, ferroelectric properties of the $RMnO_3$ compounds.

IV. CONCLUSIONS

$NdMnO_3$ manganite has been investigated by neutron diffraction, neutron depolarization, dc magnetization, and ac susceptibility techniques. A canted AFM type ordering among Mn moments sets in below 73 K. Ordering of Nd moments below 15 K induces a reorientation (by 180°) of net FM moment of Mn ions along b axis. This reorientation causes the reversal of the net magnetic moment opposite to the applied magnetic field below 15 K. The Nd sublattice ordering, below 15 K, has remarkable effects on magnetostructural coupling and magnetocaloric effect. The present investigation of the magnetic properties on single phase stoichiometric $NdMnO_3$ compound gives an atomic level understanding of the low temperature magnetic ordering as well as of the magnetization reversal phenomenon in this interesting perovskite compound. The observed magnetostructural coupling, at the Nd magnetic sublattice ordering, is interesting from the point of view of the practical applications of such perovskites in magnetostrictive transducers. The present finding is significant as it would generate new interest in $RMnO_3$ compounds to investigate the role of rare-earth (of larger size) magnetic ordering and the coupled structural distortions on their various physical properties, such as magnetocaloric effect, thermoelectric effect, dielectrics, and ferroelectricity.

[1] J. G. Bednorz and K. A. Müller, Rev. Mod. Phys. **60**, 585 (1988).
[2] A. P. Ramirez, J. Phys.: Condens. Matter **9**, 8171 (1997).
[3] B. Madhavan and A. Ashok, Ionics **21**, 601 (2015).
[4] N.-G. Park, Mater. Today **18**, 65 (2015).
[5] N. Nuraje and K. Su, Nanoscale **5**, 8752 (2013).
[6] P. K. Panda, J. Mater. Sci. **44**, 5049 (2009).
[7] C. N. R. Rao, J. Phys. Chem. B **104**, 5877 (2000).
[8] Y. Tokura, *Colossal Magnetoresistive Oxides* (CRC, Boca Raton, FL, 2000).
[9] B. Lorenz, ISRN Condens. Matter Phys. **2013**, 43 (2013).
[10] J. H. Park, E. Vescovo, H. J. Kim, C. Kwon, R. Ramesh, and T. Venkatesan, Nature (London) **392**, 794 (1998).
[11] C. N. R. Rao and B. Raveau, *Colossal Magnetoresistance, Charge Ordering and Related Properties of Manganese Oxides* (World Scientific, Singapore, 1998).
[12] J. A. Alonso, M. J. Martínez-Lope, M. T. Casais, and M. T. Fernández-Díaz, Inorg. Chem. **39**, 917 (2000).
[13] S. Quezel, F. Tcheou, J. Rossat-Mignod, G. Quezel, and E. Roudaut, Physica B+C **86-88**, 916 (1977).
[14] T. Lonkai, D. Hohlwein, J. Ihringer, and W. Prandl, Appl. Phys. A **74**, s843 (2002).
[15] J. Park, U. Kong, S. I. Choi, J.-G. Park, C. Lee, and W. Jo, Appl. Phys. A **74**, s802 (2002).
[16] T. Kimura, G. Lawes, T. Goto, Y. Tokura, and A. P. Ramirez, Phys. Rev. B **71**, 224425 (2005).
[17] R. Feyerherm, E. Dudzik, O. Prokhnenko, and D. N. Argyriou, J. Phys. Conf. Ser. **200**, 012032 (2010).
[18] W. S. Ferreira, J. Agostinho Moreira, A. Almeida, M. R. Chaves, J. P. Araújo, J. B. Oliveira, J. M. Machado Da Silva, M. A. Sá, T. M. Mendonça, P. Simeão Carvalho, J. Kreisel, J. L. Ribeiro, L. G. Vieira, P. B. Tavares, and S. Mendonça, Phys. Rev. B **79**, 054303 (2009).
[19] T. Kimura, T. Goto, H. Shintani, K. Ishizaka, T. Arima, and Y. Tokura, Nature (London) **426**, 55 (2003).
[20] O. Prokhnenko, R. Feyerherm, E. Dudzik, S. Landsgesell, N. Aliouane, L. C. Chapon, and D. N. Argyriou, Phys. Rev. Lett. **98**, 057206 (2007).
[21] S. Nandi, A. Kreyssig, L. Tan, J. W. Kim, J. Q. Yan, J. C. Lang, D. Haskel, R. J. McQueeney, and A. I. Goldman, Phys. Rev. Lett. **100**, 217201 (2008).
[22] A. Kumar and S. M. Yusuf, Phys. Rep. **556**, 1 (2015).
[23] H. Adachi and H. Ino, Nature (London) **401**, 148 (1999).

[24] S. M. Yusuf, A. Kumar, and J. V. Yakhmi, Appl. Phys. Lett. **95**, 182506 (2009).

[25] P. Mandal, A. Sundaresan, C. N. R. Rao, A. Iyo, P. M. Shirage, Y. Tanaka, C. Simon, V. Pralong, O. I. Lebedev, V. Caignaert, and B. Raveau, Phys. Rev. B **82**, 100416 (2010).

[26] J. Krishna Murthy and A. Venimadhav, Physica B **448**, 162 (2014).

[27] J. Mao, Y. Sui, X. Zhang, Y. Su, X. Wang, Z. Liu, Y. Wang, R. Zhu, Y. Wang, W. Liu, and J. Tang, Appl. Phys. Lett. **98**, 192510 (2011).

[28] S. Cao, H. Zhao, B. Kang, J. Zhang, and W. Ren, Sci. Rep. **4**, 5960 (2014).

[29] K. Yoshii, M. Mizumaki, K. Matsumoto, S. Mori, N. Endo, H. Saitoh, D. Matsumura, T. Kambe, and N. Ikeda, J. Phys.: Conf. Series **428**, 012032 (2013).

[30] T. Bora and S. Ravi, J. Magn. Magn. Mater. **386**, 85 (2015).

[31] P. Gupta and P. Poddar, Inorg. Chem. **54**, 9509 (2015).

[32] V. A. Cherepanov, L. Y. Barkhatova, A. N. Petrov, and V. I. Voronin, J. Solid State Chem. **118**, 53 (1995).

[33] I. O. Troyanchuk, V. A. Khomchenko, S. N. Pastushonok, O. A. Novitsky, V. I. Pavlov, and H. Szymczak, J. Magn. Magn. Mater. **303**, 111 (2006).

[34] N. Ihzaz, M. Boudard, H. Vincent, and M. Oumezzine, J. Alloy. Compd. **479**, 445 (2009).

[35] N. Ihzaz, H. Vincent, G. Dezanneau, H. Roussel, J. Dhahri, and M. Oumezzine, J. Magn. Magn. Mater. **281**, 221 (2004).

[36] F. Bartolomé, J. Bartolomé, and J. Campo, Physica B **312–313**, 769 (2002).

[37] F. Bartolome, J. Herrero-Albillos, L. M. Garcia, J. Bartolome, N. Jaouen, and A. Rogalev, J. Appl. Phys. **97**, 10A503 (2005).

[38] M. Mihalik jr., M. Mihalik, S. Maťaš, and M. Vavra, Acta Phys. Pol. A **126**, 284 (2014).

[39] E. T. Maguire, A. M. Coats, J. M. S. Skakle, and A. R. West, J. Mater. Chem. **9**, 1337 (1999).

[40] I. O. Troyanchuk, Phys. Solid State **48**, 898 (2006).

[41] F. Hong, Z. Cheng, J. Wang, X. Wang, and S. Dou, Appl. Phys. Lett. **101**, 102411 (2012).

[42] T. Chatterji, B. Ouladdiaf, and D. Bhattacharya, J. Phys.: Condens. Matter **21**, 306001 (2009).

[43] S. Chandra, A. Biswas, M. H. Phan, and H. Srikanth, J. Magn. Magn. Mater. **384**, 138 (2015).

[44] T. Mori, N. Kamegashira, K. Aoki, T. Shishido, and T. Fukuda, Mater. Lett. **54**, 238 (2002).

[45] B. Dabrowski, S. Kolesnik, A. Baszczuk, O. Chmaissem, T. Maxwell, and J. Mais, J. Solid State Chem. **178**, 629 (2005).

[46] S. Y. Wu, C. M. Kuo, H. Y. Wang, W.-H. Li, K. C. Lee, J. W. Lynn, and R. S. Liu, J. Appl. Phys. **87**, 5822 (2000).

[47] A. Muñoz, J. A. Alonso, M. J. Martínez-Lope, J. L. García-Muñoz, and M. T. Fernández-Díaz, J. Phys.: Condens. Matter **12**, 1361 (2000).

[48] J. Hemberger, M. Brando, R. Wehn, V. Y. Ivanov, A. A. Mukhin, A. M. Balbashov, and A. Loidl, Phys. Rev. B **69**, 064418 (2004).

[49] S. Baran, V. Dyakonov, T. Hofmann, A. Hoser, B. Penc, Z. Kravchenko, and A. Szytuła, J. Magn. Magn. Mater. **344**, 68 (2013).

[50] N. V. Kasper and I. O. Troyanchuk, J. Phys. Chem. Solids **57**, 1601 (1996).

[51] J. S. Zhou and J. B. Goodenough, Phys. Rev. B **68**, 144406 (2003).

[52] T. Goto, T. Kimura, G. Lawes, A. P. Ramirez, and Y. Tokura, Phys. Rev. Lett. **92**, 257201 (2004).

[53] V. Dyakonov, F. N. Bukhanko, V. I. Kamenev, E. E. Zubov, M. Arciszewska, W. Dobrowolski, V. Mikhaylov, R. Puźniak, A. Wiśniewski, K. Piotrowski, V. Varyukhin, H. Szymczak, A. Szytuła, R. Duraj, N. Stüsser, A. Arulraj, S. Baran, B. Penc, and T. Jaworska-Gołąb, Phys. Rev. B **77**, 214428 (2008).

[54] J. G. Cheng, Y. Sui, Z. N. Qian, Z. G. Liu, X. Q. Huang, J. P. Miao, Z. Lu, X. J. Wang, and W. H. Su, Wuli Xuebao/Acta Phys. Sin. **54**, 4359 (2005).

[55] W. H. Li, S. Y. Wu, K. C. Lee, and J. W. Lynn, Physica B **276–278**, 724 (2000).

[56] O. Halpern and T. Holstein, Phys. Rev. **59**, 960 (1941).

[57] S. M. Yusuf and L. M. Rao, Pramana - J. Phys. **47**, 171 (1996).

[58] H. Rietveld, J. Appl. Crystallogr. **2**, 65 (1969).

[59] A. Nandy, A. Roychowdhury, D. Das, and S. K. Pradhan, Powder Technol. **254**, 538 (2014).

[60] S. Mitsuda, H. Yoshizawa, and Y. Endoh, Phys. Rev. B **45**, 9788 (1992).

[61] M. Halder, A. K. Bera, A. Kumar, L. Keller, and S. M. Yusuf, J. Alloy. Compd. **592**, 86 (2014).

[62] S. M. Yusuf, K. R. Chakraborty, A. Kumar, A. Jain, V. Siruguri, and P. D. Babu, Neutron News **25**, 22 (2014).

[63] M. Halder, S. M. Yusuf, A. Kumar, A. K. Nigam, and L. Keller, Phys. Rev. B **84**, 094435 (2011).

[64] S. M. Yusuf, K. R. Chakraborty, S. K. Paranjpe, R. Ganguly, P. K. Mishra, J. V. Yakhmi, and V. C. Sahni, Phys. Rev. B **68**, 104421 (2003).

[65] J. M. De Teresa, C. Ritter, P. A. Algarabel, S. M. Yusuf, J. Blasco, A. Kumar, C. Marquina, and M. R. Ibarra, Phys. Rev. B **74**, 224442 (2006).

[66] M. Kaustuv, D. Samal, A. K. Bera, E. Suja, S. M. Yusuf, and P. S. A. Kumar, J. Phys.: Condens. Matter **26**, 016002 (2014).

[67] J. Rodríguez-Carvajal, in *Commission on Powder Diffraction (IUCr)*, 2001, p. 12.

[68] L. Néel, Ann. Phys. (Paris) **12**, 137 (1948).

[69] L. Néel, Adv. Phys. **4**, 191 (1955).

[70] A. Kumar, S. M. Yusuf, L. Keller, and J. V. Yakhmi, Phys. Rev. Lett. **101**, 207206 (2008).

[71] Y. Ren, T. T. M. Palstra, D. I. Khomskii, E. Pellegrin, A. A. Nugroho, A. A. Menovsky, and G. A. Sawatzky, Nature (London) **396**, 441 (1998).

[72] S.-i. Ohkoshi, K.-i. Arai, Y. Sato, and K. Hashimoto, Nat. Mater. **3**, 857 (2004).

[73] P. D. Kulkarni, U. V. Vaidya, V. C. Rakhecha, A. Thamizhavel, S. K. Dhar, A. K. Nigam, S. Ramakrishnan, and A. K. Grover, Phys. Rev. B **78**, 064426 (2008).

[74] P. Mandal, C. R. Serrao, E. Suard, V. Caignaert, B. Raveau, A. Sundaresan, and C. N. R. Rao, J. Solid State Chem. **197**, 408 (2013).

[75] P. Mandal, V. S. Bhadram, Y. Sundarayya, C. Narayana, A. Sundaresan, and C. N. R. Rao, Phys. Rev. Lett. **107**, 137202 (2011).

[76] J. L. García-Muñoz, J. Padilla-Pantoja, X. Torrelles, J. Blasco, J. Herrero-Martín, B. Bozzo, and J. A. Rodríguez-Velamazán, Phys. Rev. B **94**, 014411 (2016).

[77] M. Fiebig, T. Lottermoser, and R. V. Pisarev, J. Appl. Phys. **93**, 8194 (2003).

[78] I. Munawar and S. H. Curnoe, J. Phys.: Condens. Matter **18**, 9575 (2006).

[79] F. Yen, C. dela Cruz, B. Lorenz, E. Galstyan, Y. Y. Sun, M. Gospodinov, and C. W. Chu, J. Mater. Res. **22**, 2163 (2007).

[80] C. A. da Silva, R. S. Silva, E. J. R. Plaza, and N. O. Moreno, J. Supercond. Nov. Magn. **26**, 2497 (2013).

[81] J. S. Zhou and J. B. Goodenough, Phys. Rev. Lett. **96**, 247202 (2006).

[82] S. Samantaray, D. K. Mishra, S. K. Pradhan, P. Mishra, B. R. Sekhar, D. Behera, P. P. Rout, S. K. Das, D. R. Sahu, and B. K. Roul, J. Magn. Magn. Mater. **339**, 168 (2013).